Mechanical and Aerospace Engineering
P. Daponte (Ed.)

doi:10.3233/ATDE250335

Numerical Investigation on Pendulum Geometric Throat Matching Characteristics of Dual-Mode Ramjet Combustor

Kai Zhang[a] Duo Zhang[a] Fei Qin[a] Xuanfei Yu[a]
[a] *School of Astronautics, Northwestern Polytechnical University Xi'an China*

Abstract. FABRE (Fan Augmented Air-Breathing Ramjet Engine) represents a hypersonic combined cycle power system with extensive applications in the aerospace industry, particularly in TSTO scenarios, capable of achieving speeds up to Mach 7. However, a persistent challenge lies in achieving optimal flow matching at high Mach numbers within the FABRE dual-mode scramjet combustor, characterized by a low length-to-diameter ratio. To address this challenge, this study employs numerical simulations to scrutinize the flow dynamics within the FABRE ramjet combustor across varying geometric throat areas at Mach 7, culminating in the derivation of a matching law between the geometric throat and the isolator. The findings underscore that insufficient throat area causes inlet issues despite efficient combustion. At 89% throat area, combustion efficiency peaks with improved total temperature. Optimal efficiency is around 89% throat area. Throat area from 22% to 67% enables subsonic combustion; beyond 67%, it shifts towards supersonic combustion. Subsonic combustion sees reduced thrust and specific impulse with increased throat area, while supersonic combustion shows the opposite trend. Prioritize the 22% throat area for performance or the 100% for lower thermal protection needs. This investigation elucidates crucial insights into the geometric throat matching characteristics of hypersonic combustors, thus furnishing valuable support for future advancements in aerospace propulsion systems.

Keywords. Dual-mode Ramjet, Geometric Throat, Matching law

1. Introduction

Developing aerospace technologies, including reusable space shuttle vehicles and hypersonic aircraft, stands as a crucial objective for nations worldwide. A pivotal approach toward realizing these objectives involves leveraging the strengths of diverse traditional engines[1] to achieve enhanced combined power across the entire speed spectrum. FABRE, shown in Fig.1, a cutting-edge triple-combination power system capable of horizontal takeoff, accelerated ascent, and hypersonic cruising. Operating in turbocharged mode at low speeds and ramjet mode at high speeds, FABRE represents a versatile solution. Central to FABRE's functionality is the adjustable geometric throat, a key component designed to optimize performance by synchronizing aerodynamic parameters between the inlet and combustor across various flight conditions. By dynamically adjusting the geometric throat, the engine attains superior performance output, ensuring efficiency and effectiveness across a range of operational scenarios. This adaptive approach underscores FABRE's adaptability and underscores its potential to revolutionize aerospace propulsion systems.

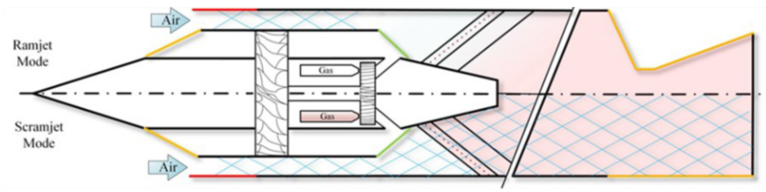

Figure 1. Schematic Diagram of FABRE.

Numerous researchers have delved into the realm of adjustable geometry throat engines, yielding valuable insights. Trefny et al. [2] utilized Ramjet Performance Analysis software (RJPA) to assess ramjet modes Ma2.5~Ma6 with thermal and mechanical choking. Their findings revealed a noteworthy 6 % ~ 8 % improvement in combustor performance with a geometric throat compared to a thermal one. Importantly, the variable geometry throat scheme maintains a fixed fuel injection position across different flight Mach numbers, thus shortening the combustor length by eliminating the need for multi-stage injection. Ortwerth [3] and colleagues conducted ground zero-speed tests on the Strutjet engine, observing enhanced engine thrust in the ejector mode with a geometric throat configuration. Comar et al. investigated the variable geometry throat characteristics of DARCO [4, 5] in RBCC engines, adjusting the throat to match heating ratio variations in different flow states for efficient combustion. Olds et al. [6] proposed the Supersonic Core Air-enhanced Thrust engine (SCAAT), utilizing Movablethroat technology to adjust the combustor throat area for efficient operation across various inflow conditions. Donohued et al. [7] explored the working characteristics of a cavity flame stabilizer using geometric choking, which accurately controls the choking position and decouples combustion heat release from pressure increase effects caused by thermal choking. Si Baranovsky [8] investigated the influence of a throttle on dual-mode ramjets, employing ground direct connection experiments to block the combustor exit with a throttle device. Bouchez et al. [9] designed the movable geometric combustor, PIAF, conducting ground direct connection experiments mirroring WRR prototype conditions. Feng [10, 11]and collaborators studied the dual-mode ramjet configuration derived from the PIAF engine, exploring hysteresis characteristics, flow field attributes, combustor losses, and the influence of slider inclination angle on combustor performance. Additionally, NASA developed the axisymmetric ejector-ramjet engine (DRACO) utilizing hydrocarbon fuel, capable of operating in three different modes. These studies collectively contribute to advancing the understanding of adjustable geometry throat engines, paving the way for enhanced aerospace propulsion technologies.

Nonetheless, limited attention has been devoted to investigating the impact of varied geometric throat areas on the combustor of the FABRE engine at high speeds. In this study, we delve into the direct connection combustion model under diverse geometric throat areas through numerical simulations, aligning with the flight conditions of FABRE ramjet mode Mach7. These findings furnish valuable insights into the geometric throat matching technology of ramjet combustors, thereby contributing to the advancement of aerospace propulsion systems.

2. Modeling

2.1. Numerical Method

In this investigation, SST k−ω turbulence model in FLUENT was utilized to solve the Reynolds-averaged Navier-Stokes equation. Discrete terms were managed by a coupled algorithm and second-order upwind scheme. The reaction dynamics of kerosene/air utilized the C10H22 molecule and a 10-step, 11-component kinetic model. The fuel injection employed ring injection with 30 spray holes on each strut side, utilizing the Taylor Analogy Breakup (TAB) model for droplet breakup. Gas phase flow utilized the Euler method, while liquid secondary fuel injection employed the Lagrange method to track droplet movement, calculating trajectory, mass, and heat transfer.

The gas mixture density in the combustor was computed via the ideal gas law, while specific heat at constant pressure was determined using mixture theory. Thermal conductivity and viscosity were derived using the ideal gas mixture law, and mass diffusion rate was calculated employing kinetic theory. For a single gas component, specific heat at constant pressure was represented by a piecewise polynomial function of temperature.

2.2. Geometry Description

In this study, the equipment throat simulates the outlet parameters of the engine inlet, proceeding to the combustor, while the tail nozzle adopts the pendulum cone geometric throat. The schematic diagram of computational combustor model is illustrated below.

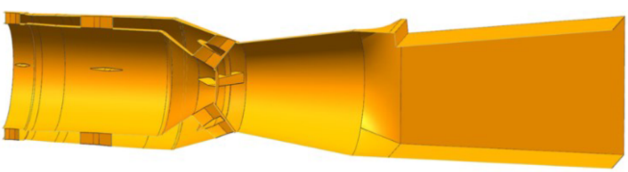

Figure 2. Geometrical Model of FABRE Combustor at 89% throat area.

The table below outlines the boundary conditions for numerical simulation. The air inlet employs mass flow rate inlet, while the outlet opts for pressure outlet.

Table 1. Inflow Conditions Setting

Inlet air mass flow rate/(kg/s)	Air inlet total temperature/(K)	Kerosene mass flow rate/(g/s)
4.46	2149	312

Table 2 illustrates the geometric throat areas corresponding to different geometric throat schemes.

Table 2. Geometric Throat Area Distribution

Scheme	A	B	C	D	E	F
Geometric throat area ratio	13%	22%	44%	67%	89%	100%

2.3. Numerical Validation

The numerical model employed in this study has undergone experimental validation in a scaled-down multi-mode combustor. Fig.3 illustrates pressure distribution curves along the combustor flowpath in two modes, revealing minimal discrepancies between numerical simulations and experimental results. This attests to the robust feasibility of the numerical method.

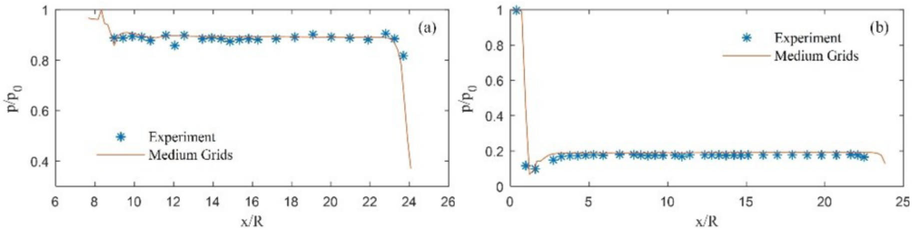

Figure 3. Validation of Pressure Distributions along Flow-Path: (a) Turbocharged Mode (b) Ramjet Mode.

3. Results And Discussion

3.1. Impact of Throat Area on Flow Field Structures

3.1.1. Impact on Mach Number Distribution

As shown in Fig.4 the contours illustrate the variation of Mach number in the combustor with different geometric throat areas.

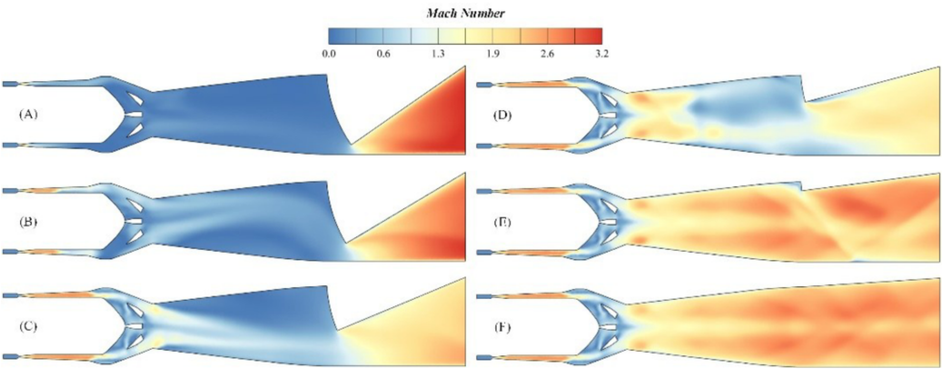

Figure 4. Mach Number Distributions with Different Throat Area.

In Scheme A, the geometric throat area is excessively small, resulting in ejection of the shock train from the isolator and subsequent failure of inlet initiation. Examining Schemes B, C, and D, reveals that increasing the geometric throat area from 22% to 44% lengthens the shock train in the isolator progressively. Further enlarging the throat area does not elongate the shock train; instead, the expansion ratio of the combustor limits its length. Observing Schemes C to F, it becomes apparent that with increasing geometric throat area, the high Mach number region within the combustor expands continuously. Notably, when the throat area changes from 67% to 89%, the Mach number within the combustor rises sharply.

3.1.2. Impact on Static Temperature Distribution

The temperature field of the combustor under various geometric throat areas is depicted in Fig.5. At 14% throat area, the combustor reaches its highest temperature. Within the 14%~44% range, temperature distribution becomes uniform, accompanied by predominantly subsonic velocities, ensuring complete combustion and elevated temperatures. With a 67% throat area, the supersonic region expands, leading to a coexistence of scramjet and sub-scramjet states within the combustor.

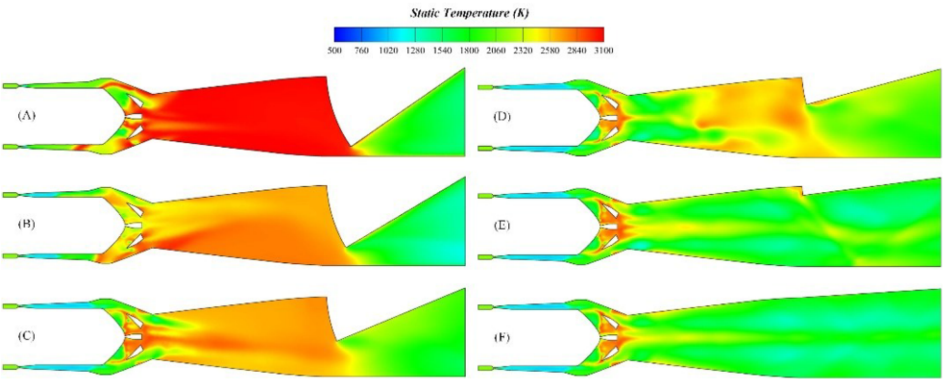

Figure 5. Static Temperature Distributions with Different Throat Area.

Notably, the high-temperature zone ahead of the geometric throat surpasses that behind the blunt body of the strut, indicating the superior flame stabilizing effect of the geometric throat in this configuration. At 89% throat area, the geometric throat induces oblique shock waves and a low-speed backflow zone. Although a high-temperature zone emerges in the backflow zone and oblique shock wave, its area is significantly smaller than the high-temperature zone behind the strut's blunt body, highlighting the superior flame stabilizing effect of the latter at this juncture.

Under 100% throat area, the combustor operates predominantly in a supersonic regime, with the high-temperature zone concentrated behind the blunt body of the strut and at the larger expansion wall surface. The strut's blunt body primarily facilitates flame stabilization in this condition.

Observing the entire throat height change process’s impact on the combustor’s temperature distribution reveals a decrease in average temperature with increasing throat height. Thus, the geometric throat plays a pivotal role in affecting the flow field's static temperature.

3.1.3. Impact on Total Temperature Distribution

In the combustion flow field, static temperature reflects the chemical energy converted into internal energy, but not kinetic energy.

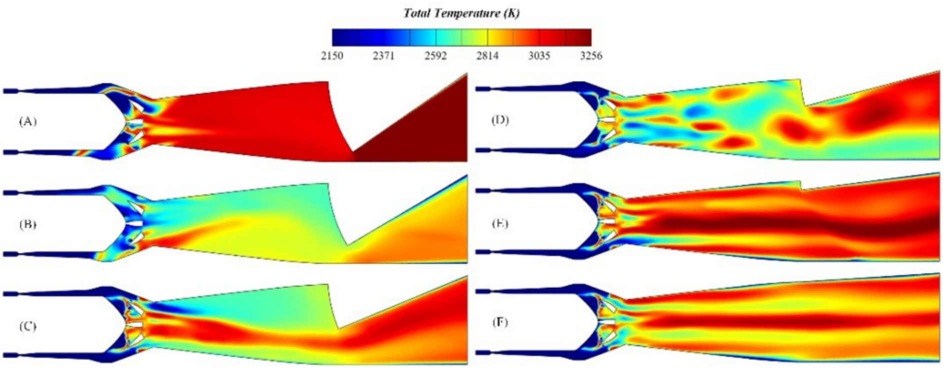

Figure 6. Total Temperature Distributions with Different Throat Area.

Total temperature, however, depicts changes in both energy and kinetic energy, providing a comprehensive view of chemical energy conversion. Fig.6 illustrates the total temperature distribution as the geometric throat area varies. Total temperature at the combustor exit rises with increasing throat height of the tail nozzle within the 22%-89% geometric throat area range. At 100% throat area, combustor velocity increases, posing combustion challenges, resulting in decreased total temperature. This observation underscores the intricate relationship between geometric throat area, combustion efficiency, and total temperature dynamics within the flow field.

3.1.4. Impact on Static Pressure Distribution

The static pressure field of the combustor, as influenced by changes in the geometric throat area, is depicted in Fig.7. Notably, the high-pressure airflow undergoes a pressure decrease and accelerates upon passing through the equipment nozzle. However, alterations in the geometric throat area cause pressure to increase as airflow passes through. This induces a series of shock waves in the isolator, elevating pressure within the combustor while reducing airflow velocity proportional to shock wave intensity. Strong shock waves decelerate airflow to subsonic speeds, prompting subsonic combustion, while weaker shock waves slow airflow to supersonic speeds, leading to supersonic combustion.

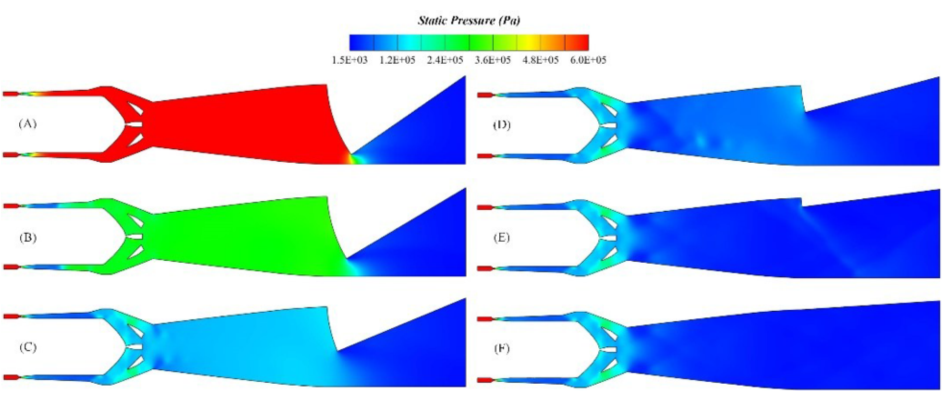

Figure 7. Static Pressure Distributions with Different Throat Area.

Within the geometric throat area range of 13% to 67%, average combustor pressure decreases with increasing throat area, with pressure influenced significantly by the tail nozzle's throat area. However, in the 67% to 100% throat area range, average combustor pressure remains relatively unchanged despite throat area adjustments, with peak pressure concentrated in the mixing section.

3.1.5. Impact on Total Pressure Distribution

Total pressure is critical for the combustor's operational capacity. As depicted in Fig.8, when the geometric throat area ranges from 13% to 44%, the combustor operates in ramjet mode. Here, the average total pressure declines with increasing height. Conversely, as the geometric throat area shifts from 44% to 100%, the combustor transitions to scramjet mode, with the average total pressure rising alongside the geometric throat height.

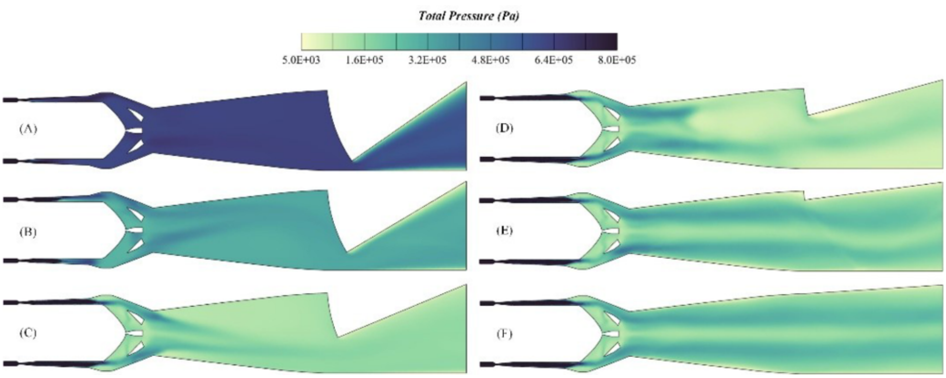

Figure 8. Total Pressure Distributions with Different Throat Area.

3.2. Impact of Throat Area on Combustion Performance

3.2.1. Combustion Efficiency Analysis

Combustion efficiency stands as a pivotal parameter gauging the conversion degree of chemical energy within the combustor. In this investigation, combustion efficiency is calculated using the total temperature rise method. The theoretical total temperature increment is derived by subtracting the air inlet total temperature from the ideal total temperature.

Meanwhile, the actual total temperature increment is obtained by subtracting the air inlet total temperature from the mass average total temperature at the nozzle inlet section. The combustion efficiency, defined by the total temperature, is compared with the theoretical total temperature increment as follows:

$$\eta_{combustion} = \frac{T_{t9} - T_{t0}}{T_{\mathrm{t}}^{\mathrm{ideal}} - T_{t0}} \tag{1}$$

T_{t9} represents the weighted average total temperature of the outlet section of the combustor, T_{t0} represents the total temperature at the inlet, and T_t^{ideal} represents the total temperature obtained by the reaction of fuel and air in an ideal state. Using the thermodynamic calculation software Cantera, the ideal total temperature of Ma7 is calculated to be 3256K. It can be seen in Scheme A of Fig.9, although the combustion efficiency is high, the pressure in the combustor is too high, and the shock wave train has moved forward out of the isolator, resulting in the intake port not starting and the engine not working normally.

In the normal working scheme of the engine except scheme A, the combustion efficiency first increases and then decreases with the increase of throat height, and reaches the maximum when the geometric throat area is 89%.

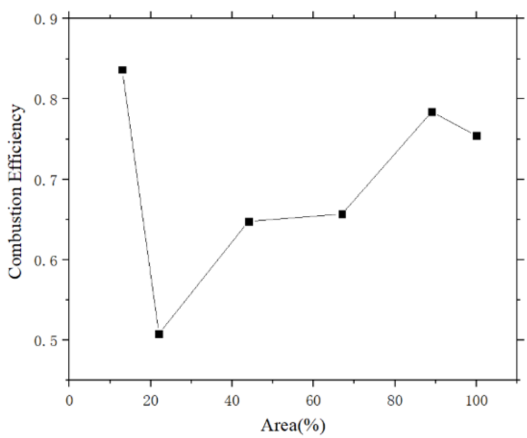

Figure 9. Combustion Efficiency with Different Throat Area.

3.2.2. Performance Analysis of Propulsion System

While combustion efficiency gauges chemical energy conversion within the combustor, it alone cannot depict overall engine performance. An engine with high combustion efficiency may not necessarily exhibit high specific impulse, and vice versa. Thus, to assess performance changes under varied geometric throat areas, we introduce an empirical inlet with a resistance coefficient of 0.17 at Mach 7. Inlet resistance is then calculated using this coefficient, and the engine's overall thrust is determined by summing the simulated thrust of the combustor and nozzle, as per the following formula.

$$F = -F_i + F_{c\&n} \quad (2)$$

Fig.10 shows the curve of engine thrust and specific impulse performance changing with geometric throat area.

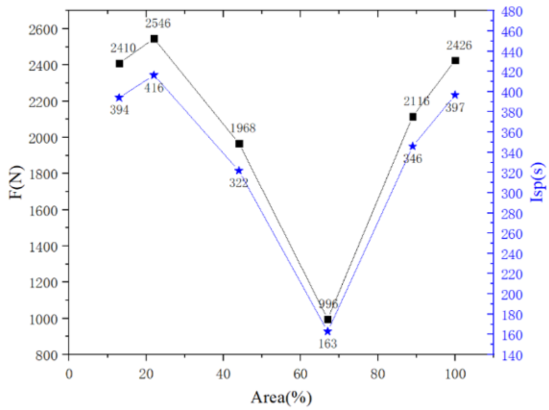

Figure 10. Thrust and Specific Impulse Performance with Different Throat Area.

By observing the curve, it can be found that the total thrust and specific impulse first decrease and then increase with the increase of geometric throat area, and the engine thrust specific impulse is the largest when the geometric throat area is 22%. At the same time, it can be observed that when the throat area is 100%, the combustor is in the scramjet mode, and the difference between the engine thrust and the maximum thrust is only 4.7%, and the difference between the specific impulse and the maximum specific impulse is only 4.6%. At the same time, because it is a scramjet mode, the thermal protection of the geometric throat is difficult, so compared with the ramjet mode with the geometric throat area of 22%, the scramjet mode with 100% geometric throat area can greatly reduce the thermal protection difficulty while maintaining it.

4. Conclusion

To investigate the impact of varying geometric throat areas on the combustor of the FABRE engine operating at high speeds, numerical simulations were conducted employing different combustion models corresponding to ramjet mode Mach 7 flight conditions. The analysis delves into the matching characteristics between geometric throat area and the multi-mode combustor, considering parameters such as Mach number, temperature, pressure, combustion efficiency, and engine performance, yielding the following key findings:

1) Insufficient geometric throat area, despite yielding high combustion efficiency, results in excessive pressure leading to the displacement of the shock train from the isolator, thereby causing inlet unstart and engine shutdown. Hence, excessively small geometric throat areas should be avoided.

2) Under normal isolator operation, expanding the geometric throat area to 89% reduces pressure and static temperature while enhancing total temperature and combustion efficiency. Further expansion beyond 89% sustains pressure while diminishing static and total temperatures along with combustion efficiency. Thus, maintaining the geometric throat area around 89% optimizes combustion efficiency.

3) Geometric throat area transitions from 22% to 67% primarily facilitate subsonic combustion. Beyond 67%, a gradual shift towards supersonic combustion occurs as the throat area increases from 67% to 100%.

4) In subsonic combustion, engine thrust and specific impulse decline with increasing geometric throat area, whereas in supersonic combustion, they exhibit an upward trend with expanding throat area.

5) Compared to peak performance in scramjet mode, engine thrust and specific impulse in ramjet decrease by 4.7% and 4.6%, respectively. However, absence of thermal protection concerns with geometric throat suggests enhanced engineering feasibility. Consequently, prioritizing performance warrants utilization of the 22% geometric throat ramjet mode, whereas emphasizing lower thermal protection requirements favors the 100% geometric throat area scramjet mode.

These insights inform strategic decision-making regarding geometric throat configurations in hypersonic combustor design, balancing performance optimization and engineering practicality.

5. Acknowledgment

The research work is supported by the National Key Laboratory Foundation of China (No. 6142704210207).

References

[1] Chhaniyara A., Cryogenic rocket engine, International Journal of Mechanical Engineering and Robotics Research, 2 (2013) 373-378.

[2] Trefny C., Dippold V., Supersonic free-jet combustion in a ramjet burner, in: 46th AIAA/ASME/SAE/ASEE Joint Propulsion Conference & Exhibit, 2010, pp. 6643.

[3] Ortwerth P., Ratekin G., Goldman A., Emanuel M., Horn M., Rocketdyne Development of RBCC Engine for Low Cost Access to Space, (1997).

[4] Komar D., McDonald J., DRACO Flowpath Performance and Environments, in, 1999.

[5] Brown T., Smith N., Reuse fo a Cold War Surveillance Drone to Flight Test a NASA Rocket Based Combined Cycle Engine, in, 1999.

[6] Olds J., Bradford J., Supersonic Core Air-Augmented Thrusting (SCAAT) Engine, in, 2013.

[7] Donohue J.M., Dual-Mode Scramjet Flameholding Operability Measurements, J. Propul. Power, 30 (2014) 592-603.

[8] BARANOVSKII S., LEVIN V., Wide-range combustion chamber of ramjet, in: 3rd International Aerospace Planes Conference.

[9] Bouchez M., Levine V., French-Russian Cooperation on Dual-Mode Ramjet: significant step passed for technology and combustion processes mastering, in: 12th AIAA International Space Planes and Hypersonic Systems and Technologies, 2003, pp. 7004.

[10] Feng S., Chang J., Zhang Y., Zhang C., Wang Y., Bao W., Numerical studies for performance improvement of a variable geometry dual mode combustor by optimizing deflection angle, Aerosp. Sci. Technol., 68 (2017) 320-330.

[11] eng S., Chang J., Zhang J., Zhang C., Bao W., Numerical and experimental investigation of improving combustion performance of variable geometry dual-mode combustor, Aerosp. Sci. Technol., 64 (2017) 213-222.